

Theoretical analysis of the Faraday effect in zigzag carbon nanotubes

Abbas Zarifi* and Thomas Garm Pedersen

Department of Physics and Nanotechnology, Aalborg University, Skjernvej 4A, DK-9220, Aalborg East, Denmark

(Received 17 August 2007; revised manuscript received 9 January 2008; published 7 February 2008)

The optical properties of zigzag carbon nanotubes in magnetic fields are analyzed. Using a tight-binding model with nearest-neighbor interactions, general expressions are computed for the diagonal and off-diagonal elements of the frequency dependent susceptibility in the presence of an axial magnetic field. The off-diagonal elements are applied to calculate the interband Faraday rotation and the Verdet constant. We predict that these effects should be clearly detectable under realistic conditions using weak magnetic fields.

DOI: [10.1103/PhysRevB.77.085409](https://doi.org/10.1103/PhysRevB.77.085409)

PACS number(s): 33.55.+b, 75.75.+a, 78.67.Ch

I. INTRODUCTION

Since 1991, the optical properties of carbon nanotubes (CNs) have been studied extensively both experimentally and theoretically.¹⁻⁹ Along with optical properties, magneto-optical phenomena, being a source of information about the electronic structure of CNs, have been investigated considerably.¹⁰⁻¹⁶ The rotation of the polarization of a plane-polarized electromagnetic wave passing through a substance under the influence of a static magnetic field along the direction of propagation is known as the Faraday rotation. Ever since it was first observed, the Faraday effect for solids, liquids, and gases has been the subject of many theoretical and experimental investigations.¹⁷⁻²³ The goal of this paper is to study the Faraday effect in single-walled zigzag CNs threaded by a parallel magnetic field. To the best of our knowledge, this is the first investigation of this effect in CNs. Neither theoretical nor experimental work has been made until now. For a weak magnetic field B and a nonoptically active solid, one can treat the Faraday effect as a first-order effect in B . We shall therefore concentrate on the low magnetic field limit to expand the off-diagonal elements of the susceptibility tensor to first order in the magnetic field and calculate the Faraday rotation as a first-order effect in B . Our findings clearly demonstrate that while the diagonal response is quite insensitive to even huge magnetic fields, rather modest fields (on the order of 1 T) lead to detectable changes in the off-diagonal response. In particular, we compute the Verdet constant of CNs in aqueous dispersions and show that under realistic conditions the CN signature should be clearly detectable above the background. The applied tight-binding method for studying the Faraday effect in zigzag CNs does not include exciton effects.

This paper is organized as follows. In Sec. II, we present a general reduced form of the Hamiltonian for zigzag CNs in the presence of an external magnetic field and analyze the corresponding eigenvalues and eigenvectors. In Sec. III, we obtain diagonal and off-diagonal elements of the optical susceptibility tensor in the presence of a magnetic field. Expanding the off-diagonal elements to first order in the mag-

netic field we obtain the Faraday rotation and the Verdet constant for zigzag CNs in Sec. IV. Finally, a summary is given in Sec. V.

II. TIGHT-BINDING FRAMEWORK

First of all, we study the electronic structure of the zigzag CNs denoted by $(n,0)$ in the usual (n,m) notation in the presence of an external magnetic field. At relatively low photon energies the optical response of CNs, treated as a rolled-up graphene sheet, is mainly due to the π electrons. This feature has been used to provide analytic expressions for the zero-magnetic-field susceptibility based on the tight-binding band structure of zigzag CNs in Ref. 24 (hereafter referred to as I) and the dielectric constant of graphite.²⁵ In addition, numerical calculations have been made by one of us²⁶ to calculate the Faraday rotation in graphite. We use this procedure and the one used in Ref. 27 as our starting point. Considering only nearest-neighbor interactions, the elements of the Hamiltonian matrix in the presence of an axial external magnetic field are given by

$$H_{\alpha\beta}^{(B)}(k) = \sum_t \exp[-i\Delta_{\alpha\beta}(t)]H_{\alpha\beta}(k), \quad (1)$$

where $H_{\alpha\beta}(k)$ are the Hamiltonian matrix elements for zero magnetic field given for the t th unit cell [the expression inside the sum in Eq. (3) of I], and where¹¹

$$\Delta_{\alpha\beta}(t) = \frac{e}{\hbar} \int_0^1 (\vec{R}_{\beta 0} - \vec{R}_{\alpha t}) \cdot \vec{A}[\vec{R}_{\alpha t} + \eta(\vec{R}_{\beta 0} - \vec{R}_{\alpha t})] d\eta. \quad (2)$$

Here, $e > 0$ is the elementary charge, $\vec{R}_{\alpha t}(\vec{R}_{\beta 0})$ is the position vector of α (β) carbon atoms in the t th (zeroth) unit cell, and \vec{A} is the vector potential associated with the magnetic field. The magnetic field $\vec{B} = B\hat{z}$ is along the nanotube axis and the symmetric gauge $\vec{A}(\vec{r}) = B/2(-y, x, 0)$ is applied. Using the phase coefficient between chains as in I, the Hamiltonian matrix \vec{H} in the presence of the magnetic field reduces to a 4×4 matrix given by

$$\vec{H} = \gamma_0 \begin{bmatrix} 0 & e^{-iq} & 0 & e^{i(q/2)}(e^{-i\Delta} + e^{i\Delta-2i\mu\pi/n}) \\ e^{iq} & 0 & e^{-i(q/2)}(e^{-i\Delta} + e^{i\Delta-2i\mu\pi/n}) & 0 \\ 0 & e^{i(q/2)}(e^{i\Delta} + e^{-i\Delta+2i\mu\pi/n}) & 0 & e^{-iq} \\ e^{-i(q/2)}(e^{i\Delta} + e^{-i\Delta+2i\mu\pi/n}) & 0 & e^{iq} & 0 \end{bmatrix}, \quad (3)$$

where $\gamma_0 = 2.89$ eV²⁸ is the nearest-neighbor transfer integral, $q = ka/\sqrt{3}$, where $a = 2.46$ Å²⁷ is the lattice constant of graphene, and $\Delta = (eBR^2/2\hbar)\sin(\pi/n) \approx eBna^2/8\pi\hbar$ is the phase factor associated with the magnetic field for nearest-neighbor atoms, where $R = na/2\pi$ is the radius of a zigzag CN. To avoid repeated terms, we use the definitions $\tilde{\mu} = \mu - n\Delta/\pi$ and $\tilde{\mu}_{c,v} = \mu_{c,v} - n\Delta/\pi$, which are applied in all the following expressions. The Hamiltonian matrix, Eq. (3), has four eigenvalues: $E_{c_l}^{(B)}(q) = -E_{v_l}^{(B)}(q) = E_l^{(B)}(q)$ ($l=1,2$), where

$$E_l^{(B)}(q) = \gamma_0 \sqrt{3 + 2 \cos(2\tilde{\mu}\pi/n) + (-1)^l 4 \cos(\tilde{\mu}\pi/n) \cos(3q/2)}. \quad (4)$$

This result has previously been obtained by others.^{12,27,29} The obtained eigenvalues demonstrate a metal-semiconductor transition depending on the magnitude of the field.²⁹ Increasing the magnitude of the field leads to an increased band gap in the metallic case and a reduced band gap for semiconductors. Using $E_{c_l}^{(B)}(q)$ and $E_{v_l}^{(B)}(q)$ to solve the eigenvector problem, the corresponding normalized eigenvectors are given by Eq. (6) in I, where

$$a_l = \frac{e^{-i\Delta} e^{iq/2} E_l^{(B)}(q) / \gamma_0}{e^{i/2(2\tilde{\mu}\pi/n + 3q)} + (-1)^l (1 + e^{i2\tilde{\mu}\pi/n})}. \quad (5)$$

Including the overlap matrix, the energy dispersion relation for the above Hamiltonian matrix is given by²⁶

$$E_{c_l, v_l}(q) = \frac{E_{c_l, v_l}^{(B)}(q) + \varepsilon_{2p}}{1 - E_{c_l, v_l}^{(B)}(q) s_0 / \gamma_0}, \quad l = 1, 2, \quad (6)$$

where $\varepsilon_{2p} = -5$ eV is the on-site energy, $s_0 = 0.1$ is the nearest-neighbor overlap integral,²⁶ and the eigenvectors are the same as those of the Hamiltonian matrix without considering overlap.

It is of some interest to discuss the role of the overlap matrix in breaking the symmetry. It is known that the magnetic field splits the degenerate bands. But if the overlap is ignored, the so-called π - π^* symmetry is still valid and therefore the eigenvalues $E_v^{(B)}$ and $E_c^{(B)}$ lie symmetrically below and above the on-site energy ε_{2p} . By including the overlap matrix, we remove the symmetry between valence and conduction bands leading to the compression of the valence bands and the expansion of the conduction bands. In Sec. III, the crucial role of the overlap in obtaining nonzero off-diagonal elements of the susceptibility and, thereby, nonzero Faraday rotation will be demonstrated. Previously, it has

been shown that orbital overlap is essential for a correct description of off-diagonal magneto-optical effects in graphite.²⁶

III. MAGNETO-OPTICAL PROPERTIES

If the constant magnetic field points along the z direction (the direction of the nanotube axis) the general form of the susceptibility tensor is given by¹⁸

$$\chi(H) = \begin{bmatrix} \chi_{xx} & \chi_{xy} & 0 \\ -\chi_{xy} & \chi_{xx} & 0 \\ 0 & 0 & \chi_{zz} \end{bmatrix}, \quad (7)$$

where, using the defined parameter q rather than wave vector k , the susceptibility elements are defined by²⁴

$$\chi_{ij}(\omega) = \frac{\sqrt{3}}{\pi \varepsilon_0 A a} \sum_{c,v} \int_{-\pi/3}^{\pi/3} \left[\frac{d_{cv}^i(q) d_{vc}^j(q)}{E_{cv}(q) + \hbar\Omega} + \frac{d_{cv}^j(q) d_{vc}^i(q)}{E_{cv}(q) - \hbar\Omega} \right] dq. \quad (8)$$

Here, the cross sectional area $A = \pi R^2$, ε_0 is the vacuum permittivity, $d_{cv}^i(q)$ are dipole moment elements for a transition between valence band v and conduction band c at wave vector k , the excitation energy is defined by $E_{cv}(q) = E_c(q) - E_v(q)$, and the complex frequency $\Omega = \omega + i\Gamma$ contains the photon frequency ω and the broadening parameter Γ . To obtain the susceptibility tensor, we first calculate the dipole moment elements. The z component of the dipole matrix element is readily given by²⁴

$$d_{c_l, v_l}^z(q) = \frac{-2ea\gamma_0^2}{\sqrt{3}E_{l_l}^2(q)} \left[\cos\left(\frac{2\tilde{\mu}\pi}{n}\right) - (-1)^l \cos\left(\frac{\tilde{\mu}\pi}{n}\right) \cos\left(\frac{3q}{2}\right) \right], \quad (9)$$

where $E_{l_l}(q) = E_{c_l}(q) - E_{v_l}(q)$. It can be shown that $d_{c_l, v_l}^z = 0$ for $l \neq l'$ and moreover, the dipole moment vanishes for transitions between bands with different μ . Figure 1 shows the z component of the momentum (P_z) matrix element for a (6, 0) CN, where $P_z = (m_e/\hbar)e E_{ll} d_{c_l, v_l}^z$ and the magnetic field $B = 1000$ T. Taking $B = 0$ and ignoring the overlap, the plot in Fig. 1 should be identical to that of Fig. 2 in I. The difference in the magnitude is because of a mistake made in I, where a factor of 1.602 (elementary charge in units of 10^{-19} C) is incorrectly missing. This error is not present in the susceptibility spectra of I, which are all correct. Using the above dipole moment element, the zz component of the susceptibility affected by the magnetic field is given by Eq. (16) in I by replacing μ with $\tilde{\mu}$.

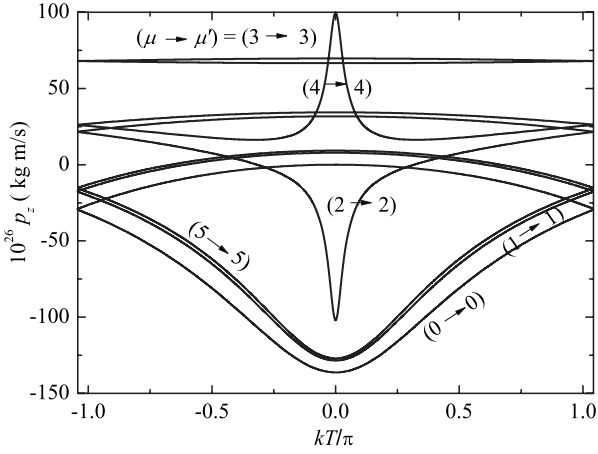


FIG. 1. k dependence of the long-axis momentum matrix elements P_z for a (6, 0) CN. All allowed interband transitions are included. The plot is for $B=1000$ T.

To find the off-diagonal elements of the susceptibility tensor, the x and y components of the dipole moment elements are required. We have found the elements of a reduced dipole matrix in the absence of magnetic field in I. In a perfectly analogous manner, a reduced dipole matrix in the presence of magnetic field will be constructed. For a right-handed rotation $\theta=x+iy$, it is found that only $\tilde{\mu}_v=\tilde{\mu}_c-1$ leads to non-zero elements given by

$$d_{14} = R\gamma_0 e^{iq/2} e^{-i\Delta} (e^{i\pi/n} - 1) (1 - e^{i\pi/n} e^{-i2\pi\tilde{\mu}_c/n}) \delta_{\tilde{\mu}_v, \tilde{\mu}_c-1},$$

$$d_{23} = d_{14}(q \rightarrow -q), \quad d_{32} = d_{41}(q \rightarrow -q), \quad d_{41} = e^{i\pi/n} d_{14}^*.$$
(10)

In the same manner for a left-handed rotation $\tilde{\theta}=x-iy$, a nonzero matrix is obtained only for $\tilde{\mu}_v=\tilde{\mu}_c+1$ that leads to

$$d_{14} = R\gamma_0 e^{iq/2} e^{-i\Delta} (e^{-i\pi/n} - 1) (1 - e^{-i\pi/n} e^{-i2\pi\tilde{\mu}_c/n}) \delta_{\tilde{\mu}_v, \tilde{\mu}_c+1},$$

$$d_{23} = d_{14}(q \rightarrow -q), \quad d_{32} = d_{41}(q \rightarrow -q), \quad d_{41} = e^{-i\pi/n} d_{14}^*.$$
(11)

We utilize Eq. (19) in I for the right-handed rotation and the similar equation for the left-handed rotation to find the dipole matrix element. Using eigenvectors \vec{c}_1 and \vec{v}_1 corresponding to the eigenvalues $E_{c_1}(q)$ and $E_{v_1}(q)$, respectively, as well as exploiting Eqs. (10) and (11) the absolute value of the dipole matrix element for the left- and right-handed operators are given by

$$|d_{c_1 v_1}^{(\pm)}| = \frac{2e\gamma_0 R}{E_{11}(q)} \left| \left[\cos\left(\frac{\tilde{\mu}_c \pi}{n}\right) - \cos\left(\frac{\tilde{\mu}_v \pi}{n}\right) \right] \sin\left(\frac{\varphi_{c_1} + \varphi_{v_1} - q}{2}\right) \right| \delta_{\tilde{\mu}_v, \tilde{\mu}_c \pm 1},$$
(12)

and a similar equation is obtained for eigenvectors \vec{c}_2 and \vec{v}_2 . Here, the relative arguments $\varphi_{c,v}$ are given by²⁴

$$\varphi_{c_1 v_1} = \arctan \left(\frac{2 \cos\left(\frac{\tilde{\mu}_{c,v} \pi}{n}\right) \sin\left(\frac{q}{2}\right) - (-1)^l \sin(q)}{2 \cos\left(\frac{\tilde{\mu}_{c,v} \pi}{n}\right) \cos\left(\frac{q}{2}\right) + (-1)^l \cos(q)} \right).$$
(13)

Using Eq. (12), the x and y components of the dipole matrix element and the xx component of the susceptibility tensor are given by Eqs. (27) and (29) in I, respectively, by replacing μ with $\tilde{\mu}$. By even taking a very large magnetic field, it is found that the diagonal susceptibility is quite insensitive to the magnetic perturbation. Because χ_{xx} is nonzero even if $B=0$, the magnetic field leads to a very small relative change in the response. In contrast, the off-diagonal susceptibility χ_{xy} vanishes in the absence of a magnetic field. In the Faraday geometry, the off-diagonal response produces a rotation of the polarization vector. By measuring this rotation experimentally, magnetic perturbations can be detected even if the diagonal response is practically unchanged. Below we demonstrate that the Faraday rotation is indeed detectable under realistic conditions using low magnetic fields.

To clarify the role of the overlap matrix, we use the defined right- and left-handed operators and express Eq. (8) in the form

$$\chi_{xy}(\omega) = \frac{\sqrt{3}\hbar\Omega}{\pi i \epsilon_0 A a} \sum_{c,v} \int_0^{\pi/3} \left[\frac{|d_{cv}(\mu_v = \mu_c - 1)|^2}{E_{cv}^2(\mu_v = \mu_c - 1) - \hbar^2 \Omega^2} - \frac{|d_{cv}(\mu_v = \mu_c + 1)|^2}{E_{cv}^2(\mu_v = \mu_c + 1) - \hbar^2 \Omega^2} \right] dq.$$
(14)

Although the overlap matrix removes the $\pi \rightarrow \pi^*$ symmetry between v and c bands, the dipole matrix elements for the left- and right-handed operators are equal and, moreover, in the case $B=0$ the allowed transition energies for the two cases are the same. Therefore, Eq. (14) is identically zero for $B=0$. The degeneracy between the transition energies is removed by the magnetic field because of the removal of symmetry by including the overlap, and then a nonzero off-diagonal susceptibility is obtained. Considering only the transition $v_1 \rightarrow c_1$, Eq. (14) yields

$$\chi_{xy}^{(\mp)}(\omega, B) = \frac{4i\sqrt{3}e^2\hbar\Omega\gamma_0^2}{\pi^2 \epsilon_0 a} \times \sum_{\mu_v, \mu_c}^{n-1} \delta_{\tilde{\mu}_v, \tilde{\mu}_c \mp 1} \left[\cos\left(\frac{\tilde{\mu}_c \pi}{n}\right) - \cos\left(\frac{\tilde{\mu}_v \pi}{n}\right) \right]^2 \times \int_0^{\pi/3} \sin\left(\frac{\varphi_{c_1} + \varphi_{v_1} - q}{2}\right)^2 \times \frac{dq}{E_{11}^2(q)[E_{11}^2(q) - \hbar^2 \Omega^2]}.$$
(15)

A similar equation is obtained for the transition $v_2 \rightarrow c_2$. After adding the expression related to the $v_2 \rightarrow c_2$ transitions to Eq. (15), the total off-diagonal element of the susceptibility tensor is given by $\chi_{xy}(\omega, B) = \chi_{xy}^{(+)}(\omega, B) - \chi_{xy}^{(-)}(\omega, B)$.

IV. LINEAR ORDER OF MAGNETIC FIELD

When the external magnetic field B is weak and when the solid is not optically active, we can treat the Faraday effect as a first-order effect in B . We shall therefore restrict our calculations to weak magnetic fields. We ignore the relatively weak field dependence of the term $[\cos(\tilde{\mu}_c\pi/n) - \cos(\tilde{\mu}_v\pi/n)]^2 \sin(\varphi_c + \varphi_v - q/2)^2$, and then expand the denominator of Eq. (15) to first order in B and express the susceptibility as $\chi_{xy}(\omega, B) = [\beta^{(+)}(\omega) - \beta^{(-)}(\omega)] \times B$. Moreover, it can be shown that $\beta^{(+)}(\omega) = -\beta^{(-)}(\omega)$, and therefore one can write $\chi_{xy}(\omega, B) = 2\beta^{(+)}(\omega) \times B$. After some simplifications the field independent coefficient $\beta^{(+)}(\omega)$ is given by

$$\begin{aligned} \beta^{(+)}(\omega) = & C\Omega \sum_{\mu_v, \mu_c}^{n-1} \delta_{\mu_v, \mu_c+1} \left[\cos\left(\frac{\mu_c\pi}{n}\right) - \cos\left(\frac{\mu_v\pi}{n}\right) \right]^2 \\ & \times \sum_{l=1}^2 \int_0^{\pi/3} \sin\left(\frac{\varphi_{c_l} + \varphi_{v_l} - q}{2}\right)^2 \\ & \times \frac{[2E_{ll}^2(q) - \hbar^2\Omega^2][F(\mu_{c_l}) - F(\mu_{v_l})]}{E_{ll}^3(q)[E_{ll}^2(q) - \hbar^2\Omega^2]^2} dq, \end{aligned} \quad (16)$$

where the constant $C = -2i\sqrt{3}e^3n\gamma_0^4(1+s_0\varepsilon_{2p}/\gamma_0)/\pi^3\varepsilon_0$, arguments φ_{c_l, v_l} are defined by Eq. (13) with $B=0$, and functions F are defined by

$$F(\mu_{c_l, v_l}) = \frac{\sin(2\mu_{c, v}\pi/n) + (-1)^l \sin(\mu_{c, v}\pi/n)\cos(3q/2)}{E_{c, v}^{(0)}(1 - s_0E_{c, v}^{(0)}/\gamma_0)^2}. \quad (17)$$

Here, $E_{c, v}^{(0)}$ indicates eigenvalues Eq. (4) with $B=0$. Due to the complicated q dependence of the trigonometric terms as well as the transition energies, no analytic solution has been found for the above integral. In the form given, however, the integral is easily computed for all zigzag CNs numerically. Real (χ'_{xy}) and imaginary (χ''_{xy}) parts of the off-diagonal elements of the susceptibility tensor for (10, 0) and (20, 0) CNs are shown in Fig. 2(a) and for (11, 0) and (19, 0) CNs in Fig. 2(b). A very prominent resonance peak is observed for semiconductor zigzag CNs with odd n . Note that all results are obtained using a rather large broadening of $\hbar\Gamma=0.15$ eV.²⁴ Experimentally, the value of the broadening is highly dependent on sample quality, reflecting the degree of bundling among the nanotubes. The large value chosen here corresponds to relatively disordered (bundled) samples. However, even in this case, the magnetic features are predicted to be clearly detectable and using higher quality samples will only increase visibility.

Now we use the off-diagonal susceptibility to find the Faraday rotation and the Verdet constant. We first consider aligned zigzag CNs suspended in water. For photon energies near the fundamental resonance peak of different zigzag CNs,³⁰ the refractive index of water n' is almost four orders of magnitude larger than the absorption coefficient n'' and this ratio is further increased for energies in the visible and near-UV range.³¹ On the whole, we take $n' \approx 1.3$ for the suspension and ignore the absorption coefficient and so the Faraday rotation ϕ at low magnetic fields is given by²⁶

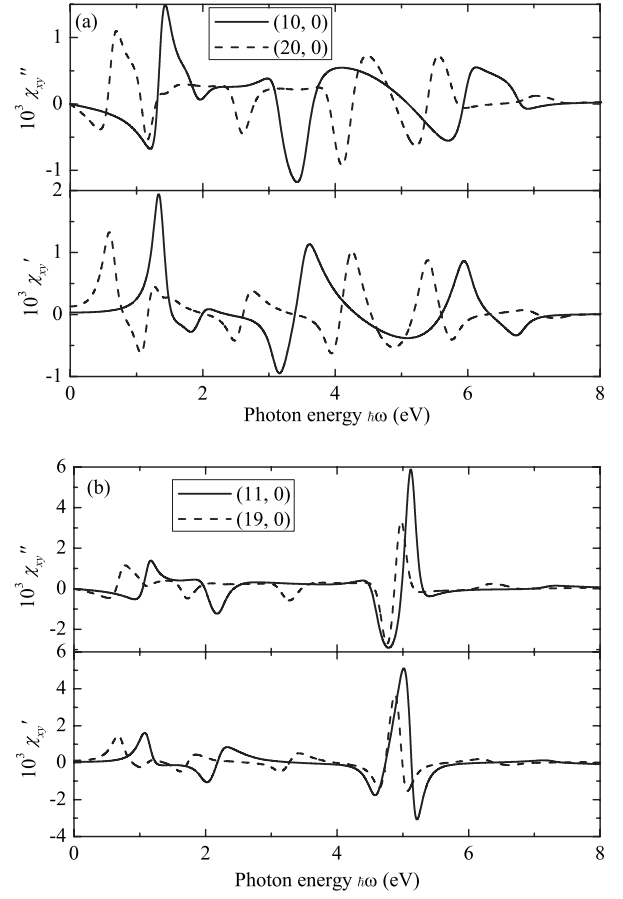


FIG. 2. Real (χ'_{xy}) and imaginary (χ''_{xy}) parts of the off-diagonal susceptibility for a magnetic field $B=1$ T. Panel (a) shows (10, 0) and (20, 0) CNs and panel (b) shows (11, 0) and (19, 0) CNs.

$$\phi = \frac{\pi d \chi''_{xy}}{\lambda n'}, \quad (18)$$

where λ is the wavelength and d is the path length. We subsequently calculate the Verdet constant V via the relation $\phi = VBd$. The energy dispersion of the Verdet constant for two groups of semiconductor CNs with even and odd n threaded by a parallel magnetic field is plotted in Figs. 3(a) and 3(b), respectively. The Verdet constant for semiconductor zigzag CNs with odd n exhibits a very prominent resonance at $\hbar\omega \approx 5$ eV and for CNs with even n two pronounced resonances around $\hbar\omega \approx 4.5$ and 5.7 eV are found. Since averaging over an ensemble of CNs would normally tend to blur individual resonances, these prominent structures are expected to prevail for ensembles containing many different semiconducting zigzag CNs.

We now address the possible experimental determination of the Verdet constant for zigzag CNs. To this end, randomly oriented CNs dispersed in water with a relative concentration of n_c is considered in order to find an averaged value of the Verdet constant. In that case, two respective rotations first about the x axis through an angle θ and secondly about the z axis through an angle φ will place a nanotube in a direction such that its axis makes an angle θ with the z axis. Therefore, the effective axial component of the magnetic field and that

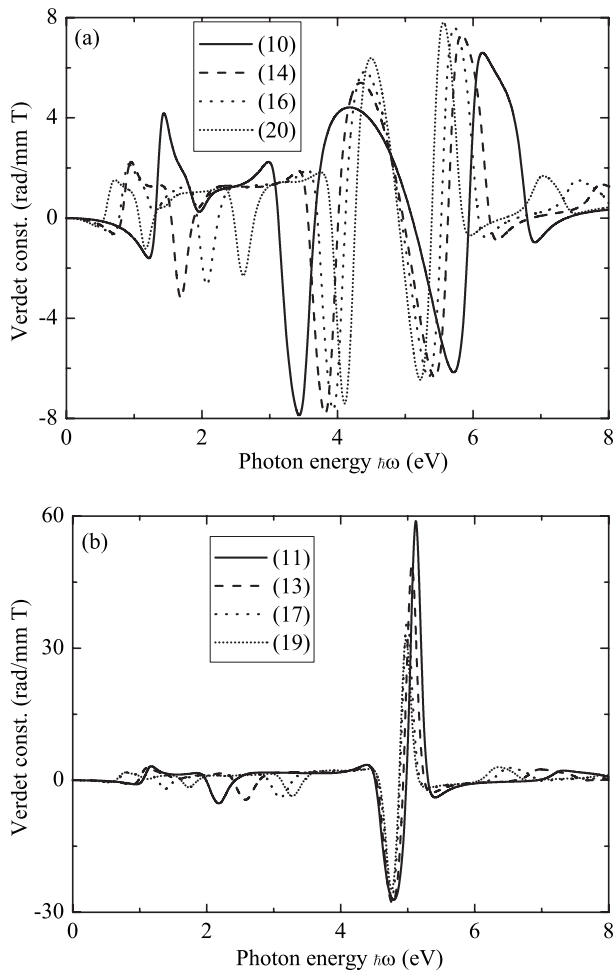


FIG. 3. Dispersion of the Verdet constant for two groups of semiconducting zigzag CNs. Panel (a) shows even n and panel (b) odd n zigzag CNs.

of the off-diagonal element of the susceptibility tensor are given by $B \cos(\theta)$ and $\chi_{xy} \cos(\varphi)^2 \cos(\theta)$, respectively. Then, by averaging, the value of the effective off-diagonal susceptibility element is equal to 1/6 of the value based on Eq. (16). Hence, including the relative concentration of CNs in the solution, the Verdet constant is given by $n_c V/6$, where V is the obtained value based on Eq. (18) for a CN threaded by a parallel magnetic field. We would like to estimate the path length for a 1° rotation of the plane of polarization of an input optical beam. For a relative concentration of $n_c=1\%$ and using the approximate value 40 rad/(mmT) for the Verdet constant of zigzag CNs with odd n and a magnetic field of 1 T, the path length obtained is as low as 0.26 mm. The Faraday rotation due to the CNs will be superimposed on a contribution from water in the suspension. However, below the optical gap of H_2O or D_2O (8.2 eV^{32,33}) very little dispersion is expected for this contribution. This is confirmed in experimental data for water in the range 1.8 to the 3.6 eV³⁴ that shows a monotonically decreasing Verdet constant with wavelength. Thus, the sharp resonances due to CNs are expected to be clearly detectable.

V. SUMMARY

A theoretical investigation based on a nonorthogonal tight-binding description has been made to study the Faraday effect in zigzag CNs. The off-diagonal elements of the susceptibility tensor under the influence of an axial external magnetic field have been calculated semianalytically and expanded to first order in the magnetic field. We have applied the obtained expressions to find the Faraday rotation and the Verdet constant of zigzag CNs. A very prominent resonance of the Verdet constant for semiconductor zigzag CNs with odd n has been demonstrated at $\hbar\omega \approx 5$ eV, which is expected to prevail for ensembles containing many different zigzag CNs. To address possible experimental verification, randomly oriented CNs suspended in water have been investigated.

*zarifi@nano.aau.dk

¹S. Tasaki, K. Maekawa, and T. Yamabe, Phys. Rev. B **57**, 9301 (1998).

²M. F. Lin, F. L. Shyu, and R. B. Chen, Phys. Rev. B **61**, 14114 (2000).

³M. Ichida, S. Mizuno, Y. Saito, H. Kataura, Y. Achiba, and A. Nakamura, Phys. Rev. B **65**, 241407(R) (2002).

⁴S. M. Bachilo, M. S. Strano, C. Kittrell, R. H. Hauge, R. E. Smalley, and R. B. Weisman, Science **298**, 2361 (2002).

⁵G. Y. Guo, K. C. Chu, D. S. Wang, and C. G. Duan, Phys. Rev. B **69**, 205416 (2004).

⁶R. Saito, A. Grüneis, G. G. Samsonidze, G. Dresselhaus, M. S. Dresselhaus, A. Jorio, L. G. Cancado, M. A. Pimenta, and A. G. S. Filho, Appl. Phys. A: Mater. Sci. Process. **78**, 1099 (2004).

⁷J. Jiang, R. Saito, A. Grüneis, G. Dresselhaus, and M. S. Dresselhaus, Carbon **42**, 3169 (2004).

⁸S. V. Goupalov, Phys. Rev. B **72**, 195403 (2005).

⁹G. Ya. Slepyan, S. A. Maksimenko, A. Lakhtakia, O. Yevtush-

enko, and A. V. Gusakov, Phys. Rev. B **60**, 17136 (1999).

¹⁰M. F. Lin and Kenneth W.-K. Shung, Phys. Rev. B **48**, 5567 (1993).

¹¹R. Saito, G. Dresselhaus, and M. S. Dresselhaus, Phys. Rev. B **50**, 14698 (1994).

¹²J. P. Lu, Phys. Rev. Lett. **74**, 1123 (1995).

¹³M. F. Lin and Kenneth W.-K. Shung, Phys. Rev. B **52**, 8423 (1995).

¹⁴H. Ajiki and T. Ando, J. Phys. Soc. Jpn. **65**, 505 (1996).

¹⁵C. C. Tsai, S. C. Chen, F. L. Shyu, C. P. Chang, and M. F. Lin, Physica E (Amsterdam) **30**, 86 (2005).

¹⁶T. Lobo, M. S. Figueira, A. Latgé, and M. S. Ferreira, Physica B **384**, 113 (2006).

¹⁷L. M. Roth, Phys. Rev. **133**, A542 (1964).

¹⁸H. S. Bennett and E. A. Stern, Phys. Rev. **137**, A448 (1965).

¹⁹M. Balkanski, E. Amzallag, and D. Langer, J. Phys. Chem. Solids **27**, 299 (1966).

²⁰M. Barthélémy and D. J. Bergman, Phys. Rev. B **58**, 12770

- (1998).
- ²¹A. V. Kimel, Y. S. Grushko, A. G. Selitskii, and A. I. Sokolov, *J. Opt. Technol.* **66**, 745 (1999).
- ²²Y. Ruan, R. A. Jarvis, A. V. Rode, S. Madden, and B. L. Davies, *Opt. Commun.* **252**, 39 (2005).
- ²³W. A. Parkinson, S. P. A. Sauer, and J. Oddershede, *J. Chem. Phys.* **98**, 487 (1993).
- ²⁴A. Zarifi and T. G. Pedersen, *Phys. Rev. B* **74**, 155434 (2006).
- ²⁵T. G. Pedersen, *Phys. Rev. B* **67**, 113106 (2003).
- ²⁶T. G. Pedersen, *Phys. Rev. B* **68**, 245104 (2003).
- ²⁷R. Saito, G. Dresselhaus, and M. S. Dresselhaus, *Physical Properties of Carbon Nanotubes* (Imperial College Press, London, 2003).
- ²⁸A. Grüneis, R. Saito, Ge. G. Samsonidze, T. Kimura, M. A. Pimenta, A. Jorio, A. G. Souza Filho, G. Dresselhaus, and M. S. Dresselhaus, *Phys. Rev. B* **67**, 165402 (2003).
- ²⁹S. Roche, G. Dresselhaus, M. S. Dresselhaus, and R. Saito, *Phys. Rev. B* **62**, 16092 (2000); J. Jiang, J. Dong, and D. Y. Xing, *ibid.* **62**, 13209 (2000); N. Y. Huang, S. D. Liang, S. Z. Deng, and N. S. Xu, *ibid.* **72**, 075412 (2005).
- ³⁰A. Zarifi, C. Fisker, and T. G. Pedersen, *Phys. Rev. B* **76**, 045403 (2007).
- ³¹G. M. Hale and M. R. Querry, *Appl. Opt.* **12**, 555 (1973).
- ³²W. Grevendonk, J. Dauwen, P. V. Keybus, and B. Vanhuysse, *J. Chem. Phys.* **81**, 3746 (1984).
- ³³L. R. Painter, R. D. Birkhoff, and E. T. Arakawa, *J. Chem. Phys.* **51**, 243 (1968).
- ³⁴A. B. Villaverde and D. A. Donatti, *J. Chem. Phys.* **71**, 4021 (1979).